A Journal of the Gesellschaft Deutscher Chemiker
Angewandte Chemie
GDCh
International Edition
www.angewandte.org

Accepted Article

Title: Facile and reversible formation of Fe(III)-O-Ce(IV) adducts from nonheme oxoiron(IV) complexes and Ce(III)

Authors: Apparao Draksharapu, Waqas Rasheed, Johannes E. M. N. Klein, and Lawrence Que

To be cited as: *Angew. Chem. Int. Ed.* 10.1002/anie.201704322
Angew. Chem. 10.1002/ange.201704322

Link to VoR: http://dx.doi.org/10.1002/anie.201704322
http://dx.doi.org/10.1002/ange.201704322

WILEY-VCH

Angewandte Chemie International Edition
10.1002/anie.201704322

Facile and reversible formation of Fe(III)–O–Ce(IV) adducts from nonheme oxoiron(IV) complexes and Ce(III)

Apparao Draksharapu, Waqas Rasheed, Johannes E. M. N. Klein, Lawrence Que, Jr.*

Dedicated to Eckard Münck in celebration of his outstanding career in bioinorganic chemistry

Abstract: *CAN or* $Ce^{IV}(NH_4)_2(NO_3)_6$ *is often used in artificial water oxidation and generally considered to be an outer-sphere oxidant. Herein we report the spectroscopic and crystallographic characterization of* $[(N4Py)Fe^{III}–O–Ce^{IV}(OH_2)(NO_3)_4]^+$ *(**3**), a complex obtained from the reaction of* $[(N4Py)Fe^{II}(NCMe)]^{2+}$ *with 2 equiv. CAN or* $[(N4Py)Fe^{IV}{=}O]^{2+}$ *(**2**) with* $Ce^{III}(NO_3)_3$ *in MeCN. Surprisingly, the formation of **3** is reversible, the position of the equilibrium being dependent on the MeCN/water ratio of the solvent. These results suggest that the* Fe^{IV} *and* Ce^{IV} *centers have comparable reduction potentials. Moreover, the equilibrium entails a change in iron spin state, from* $S = 1$ Fe^{IV} *in **2** to* $S = 5/2$ *in **3**, which is found to be facile despite the formal spin forbidden nature of this process. This observation suggests that* $Fe^{IV}{=}O$ *complexes may avail of reaction pathways involving multiple spin states having little or no barrier.*

Nature uses a Mn_4CaO_5 cluster to perform efficient water oxidation,[1] a fact that has inspired the development of artificial photosystems based on ruthenium, iridium, manganese, iron, cobalt and copper.[2] In these systems, high-valent metal-oxo species are often proposed to be the active species or precursors thereof, which are commonly generated by ceric ammonium nitrate (CAN) as a sacrificial outer-sphere oxidant.[3] However, a fleeting species has recently been identified by Lloret and Costas in a catalytic water oxidation system consisting of $[(mcp)Fe^{IV}(O)]^{2+}$ (mcp = *N,N′*-dimethyl-*N,N′*-bis(2-pyridylmethyl)-1,2-*cis*-diaminocyclohexane) and CAN in water at pH 1.[4] Based on cryo-spray mass spectrometry and resonance Raman spectroscopy, this intermediate has been formulated as $[(mcp)(O)Fe^{IV}–O–Ce^{IV}(NO_3)_3]^+$, where Ce^{IV} acts as both a Lewis acid and an inner-sphere oxidant.

The redox-inactive Ca^{2+} ion in the oxygen evolving complex (OEC) of photosystem II is essential for O–O bond formation and ultimately dioxygen generation.[5] One proposed role for the Ca^{2+} is to increase the potential of the manganese oxido cluster.[6] This notion is also in agreement with the observation that Lewis acids such as $Sc^{III}(OTf)_3$ increases the $Fe^{IV/III}$ redox potential of nonheme $Fe^{IV}{=}O$ complexes.[7] That Sc^{III} interacts directly with the $Fe^{IV}{=}O$ unit is supported by the crystal structure of $[(TMC)Fe^{III}–O–Sc^{III}(OTf)_4(solvent)]$ (TMC = 1,4,8,11-tetramethyl-1,4,8,11-tetraazacyclotetradecane) formed in the reaction of $[(TMC)Fe^{IV}(O)(NCMe)]^{2+}$ (**1**) with $Sc^{III}(OTf)_3$.[8] The corresponding reaction with $Cr^{II}(OTf)_2$ affords the $Fe^{III}–O–Cr^{III}$ adduct.[9] Here we report the reaction of $[(N4Py)Fe^{IV}(O)]^{2+}$ (**2**, N4Py = *N,N*-bis(2-pyridylmethyl)-*N*-bis(2-pyridyl)methylamine) with $Ce^{III}(NO_3)_3$ to form $[(N4Py)Fe^{III}–O–Ce^{IV}(OH_2)(NO_3)_4]^+$ (**3**) (Scheme 1). Unlike observed for the Sc- and Cr-adducts of **1**, formation of the Ce-adduct of **2** can be reversed, simply by adjusting the MeCN/water ratio of the solvent. The existence of such an equilibrium demonstrates facile electron exchange between the Fe and Ce centers, despite a formally forbidden change of spin state from $S = 1$ Fe^{IV} to $S = 5/2$ Fe^{III}. Parallel changes are also observed for $[(BnTPEN)Fe^{IV}(O)]^{2+}$ (**4**) (Scheme 1).

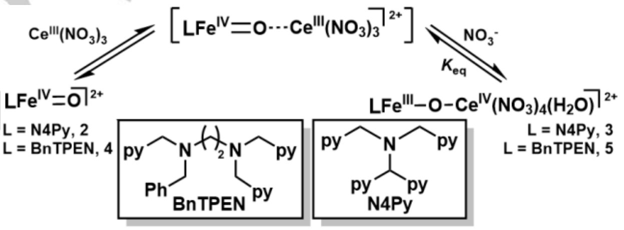

Scheme 1. Equilibria between $(L)Fe^{IV}(O)$ complexes, **2** (L = N4Py) and **4** (L = BnTPEN), and $(L)Fe^{III}–O–Ce^{IV}(NO_3)_4$ species, **3** (L = N4Py) and **5** (L = BnTPEN)

Treatment of $[(N4Py)Fe^{II}(NCMe)](OTf)_2$ in MeCN with 2 equiv. CAN in 10 µL water generates a brown species **3** with a shoulder near 500 nm (Figures 1a and S1), a result clearly distinct from that reported by Nam showing the formation of $[(N4Py)Fe^{IV}{=}O]^{2+}$ (**2**, λ_{max} 696 nm) in quantitative yield upon addition of 4 equiv. CAN to **1** in 1:3 (v/v) H_2O/MeCN.[11] Complex **3** is also formed upon addition of 4.5 equiv. $Ce(NO_3)_3$ to **2** in MeCN, resulting in the immediate loss of absorbance at 696 nm and concomitant increase at ca. 500 nm to form **3** with an isosbestic point observed at 570 nm (Figure 1b).

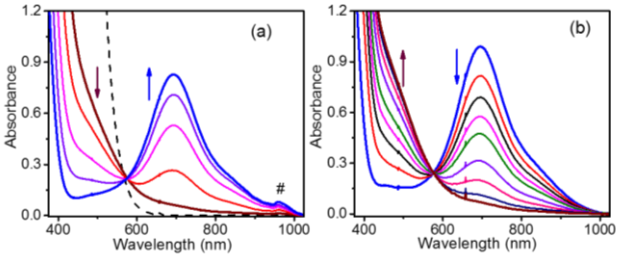

Figure 1. UV-Vis spectral changes in (a) the reaction of $[(N4Py)Fe^{II}(NCMe)]^{2+}$ (2.5 mM in MeCN, dashed line) with 2 equiv. CAN in 10 µL H_2O (solid line just above dashed line) followed by titration with water (final concentrations 2.8 M,; 3.9 M,; 5 M,; 8.3 M), resulting in increasing absorbance at 696 nm (# = vibrational overtone of water) and (b) the titration of **2** ($A_{696\ nm}$ = 1; 2.5 mM in MeCN) with $Ce^{III}(NO_3)_3$ in MeCN (0.25, 0.5, 0.75, 1, 1.5, 2, 3, 4.5 equiv.), resulting in diminishing absorbance at 696 nm.

---

[a] Dr. Apparao Draksharapu, Waqas Rasheed, Dr. Johannes E. M. N. Klein, Prof. Dr. Lawrence Que, Jr.
Department of Chemistry and Center for Metals in Biocatalysis, University of Minnesota, Minneapolis, Minnesota 55455, United States
E-mail: larryque@umn.edu

Supporting information for this article is given via a link at the end of the document.

10.1002/anie.201704322

ESI-MS analysis of **3** in MeCN reveals two major peaks at m/z 827.1 and 914.0 with masses and isotope patterns corresponding to $[(N4Py)Fe^{III}–O–Ce^{IV}(NO_3)_3(X)]^+$ ions with X = NO_3 and OTf (Figures S5-S7). In support of the iron(III) oxidation state assignment, **3** exhibits at 4 K broad EPR signals with g = 8.9 and 4.3, which are characteristic of a rhombic $S = 5/2$ Fe^{III} species (Figure S9). The resonance Raman spectrum of **3** (λ_{exc} 514.5 nm) shows an enhanced band at 707 cm^{-1} (Figure 2a) that shifts to 676 cm^{-1} upon ^{18}O labeling, the 31-cm^{-1} downshift being in excellent agreement with the calculated value based on Hooke's law of 31 cm^{-1} for a diatomic Fe–O oscillator. As the Ce atom is much heavier than the iron atom, the former would not be expected to contribute to the Fe–O stretch. For comparison, this vibration has a slightly higher frequency than that found by Borovik for $[(H_3buea)Fe^{III}(O)]^{2-}$ (671 cm^{-1}, H_3buea = tris[(N'-tert-butylureaylato)-N-ethylene]aminato)trianion).[12]

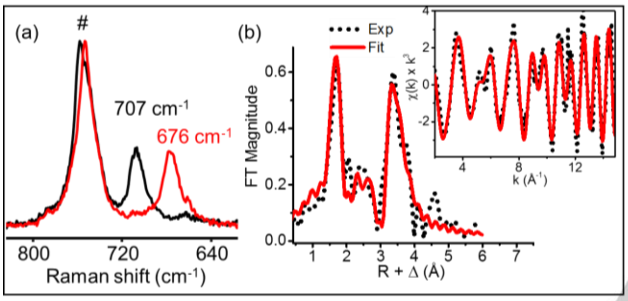

Figure 2. (a) Resonance Raman spectra (λ_{exc} 514.5 nm) of **3** from the reaction of 5 mM $[(N4Py)Fe^{II}(NCMe)]^{2+}$ in MeCN with 2.2 equiv. CAN in 10 μL H_2O (black) and the corresponding ^{18}O-labeled complex generated from 2.2 equiv. CAN in 10 μL $H_2{}^{18}O$ (red). # represents a MeCN deformation. (b) Unfiltered Fe K-edge EXAFS spectrum (dotted line) and best fit (solid line) of **3**. Inset: corresponding unfiltered k-space data (dots) and best fit (line).

To shed further light into its nature, X-ray absorption spectroscopy (XAS) studies have been carried out on frozen solutions of **3**. The Fe K-edge for **3** is observed at 7122.7 eV (Figure S12), a value comparable to those of $[(TMC)Fe^{III}–O–Sc^{III}(OTf)_4(L)]$ (7122.6 eV)[8b] and other ferric complexes.[13] Complex **3** exhibits a single pre-edge feature (assigned to a 1s → 3d transition) at 7112.9 eV with an area of 13.7 units, consistent with values found for (μ-oxo)diferric complexes.13c The Fourier transformed EXAFS spectrum of **3** shows prominent features at R + Δ ~ 1.7 and 3.4 Å (Figure 2b) corresponding to 1 N/O scatterer at 1.84 Å (the oxo bridge), 5 N/O scatterers at 2.13 Å (N4Py N-atoms) and a Ce scatterer at 3.8 Å indicating the presence of a nearly linear $Fe^{III}–O–Ce^{IV}$ core (see Table S5 for further details).

The thermal stability of **3** led to the growth of diffraction quality crystals by slow diffusion of ether into a solution of **2** (derived from the oxidation of $[(N4Py)Fe^{II}(NCMe)](ClO_4)_2)$ in the presence of 5 equiv. $Ce^{III}(NO_3)_3$ in acetonitrile at -20 ºC. The crystallographic analysis (Figure 3, Table S5) confirms the results from XAS analysis. There is a nearly linear $Fe^{III}–O–Ce^{IV}$ unit with an Fe–O–Ce angle of 170.3º, similar to the Fe–O–Fe angle (172º) found in $[(N4Py)Fe^{III}–O–Fe^{III}(N4Py)]^{4+}$.[14] Its Fe–O bond length of 1.825 Å is significantly longer than the 1.64-Å Fe=O bond of **2** but comparable to those of $[(N4Py)_2Fe^{III}{}_2(O)]^{4+}$ (1.8034(10) Å) and $[(N4Py)Fe^{III}(OCH_3)]^{2+}$ (1.77 Å).[14] In addition, the average Fe–N_{Py} bond length of 2.11 Å found for **3** is comparable to those of $[(N4Py)Fe^{III}(OCH_3)]^{2+}$ (2.11 Å) and $[(N4Py)_2Fe^{III}{}_2O]^{4+}$ (2.13 Å), both of which have high-spin ferric centers (Table S5). Lastly, **3** has an Fe⋯Ce distance of 3.825(5) Å, which is longer than those found for other $Fe^{III}–O–M$ complexes, e.g. ≤ 3.61 Å for M = Fe^{III},[9b],[14] and 3.64 for M = Sc^{III},[8] reflecting the larger ionic radius of the Ce^{IV} center.

The cerium atom in **3** is connected to the iron half of the molecule via the oxo bridge. The Ce–μ-O bond length is 2.013(2) Å, much shorter than the 2.418(2)-Å distance observed for the Ce–OH_2 bond in **3**, which is within the range of reported aquacerium(IV) complexes.[15] However the Ce–μ-O bond of **3** is longer than the $Ce^{IV}=O$ bonds observed for $(H_2O)(LOEt)_2Ce^{IV}=O$ (1.857(3) Å) (LOEt = $CpCo\{P(O)–(OEt)_2\}_3)$ and $[(N(CH_2CH_2NSi^tBuMe_2)_3)Ce^{IV}=O]^-$ (1.902(2) Å).[16] In addition, the Ce center has four κ^2-bound nitrate ligands with an average Ce–O bond length of 2.52 Å, which is consistent with the 2.508(7)-Å distance observed in CAN.[17]

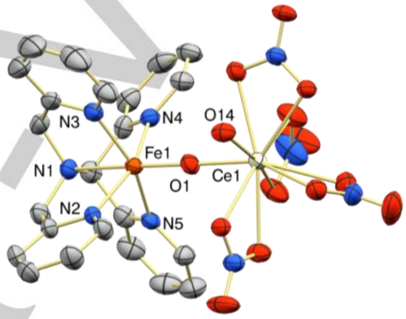

Figure 3. ORTEP plot for $[(N4Py)Fe^{III}–O–Ce^{IV}(OH_2)(NO_3)_4]^+$ (**3**) with 50% probability ellipsoids (H atoms omitted for clarity). Selected distances (Å): Fe(1)−O(1), 1.825(2); Fe(1)−N(1), 2.162(3); Fe(1)−N(2), 2.084(3); Fe(1)−N(3), 2.072(3); Fe(1)−N(4), 2.108(3); Fe(1)−N(5), 2.117(3); Ce(1)−O(1), 2.013(2); Ce(1)−O(14), 2.418(3); Ce(1)−O(nitrate), 2.518(3); Ce(1)•••Fe(1), 3.8247(5). ∠Fe(1)−O(1)−Ce(1) = 170.3(1)º. CCDC 1546446.

Unexpectedly, subsequent experiments revealed **2** and **3** to be involved in a reversible equilibrium. Figure 1a shows the effect of titrating a MeCN solution of **3** with water, where the 696-nm band associated with **2** was fully formed at a water concentration of 7.5 M, with an isosbestic point at 580 nm. Subsequent dilution of this sample with MeCN shifted the equilibrium back in favor of **3**. This conclusion was corroborated by ESI-MS experiments that showed the disappearance and re-appearance of the ions associated with **3** under the different solvent conditions concomitant with the appearance and disappearance of **2** (Figure S6). Analogous experiments with $[(BnTPEN)Fe^{IV}=O]^{2+}$ (**4**) (BnTPEN = *N*-benzyl-*N,N',N'*-tris(2-pyridylmethyl)-1,2-diaminoethane) and $Ce^{III}(NO_3)_3$ afforded $[(BnTPEN)Fe^{III}–O–Ce^{IV}(OH_2)(NO_3)_4]^+$ (**5**), with comparable properties as **3** (Figures S3, S4, S6, S9-S11, S13, S15). In contrast to **2** and **3**, the conversion of **4** to **5** required only 2 equiv. $Ce^{III}(NO_3)_3$, but more water (10 M) was needed to shift the equilibrium between **4** and **5** back in favor of **4**. The equilibria demonstrated between **2** and **3** and between **4** and **5** represent the first examples of reversible inner-sphere electron transfer between Ce^{III} and an $Fe^{IV}=O$ complex.

The existence of such equilibria suggests that the $Fe^{IV/III}$ potentials of **2** and **4** and the $Ce^{IV/III}$ potentials of **3** and **5** are not very different from each other. Where each equilibrium lies under the different conditions depends on the respective ligand

10.1002/anie.201704322

environments of the two metal centers involved. Based on our accumulated observations, **4** would appear to have a somewhat higher redox potential than **2**, as less $Ce(NO_3)_3$ is required to form **5** from **4** but more water is needed to convert **5** back to **4**. That **4** is more oxidizing than **2** is consistent with conclusions derived from comparative electrochemical data (Table 1). On the other hand, the observed shifts in the above equilibria from dry MeCN to wet MeCN reflect an increase in the $Ce^{IV/III}$ potential (Figure S20) as the nitrates bound to Ce^{IV} in **3** and **5** are progressively replaced by water.

Table 1. Redox properties of select nonheme $Fe^{IV}(O)$ complexes.[a]

	1	2	4	Refs
Reaction with $Ce^{III}(NO_3)_3$ in MeCN	No rxn	yes	yes	This work
$E_{p,c}$ by cyclic voltammetry in dry MeCN [b]	+0.08	-0.13	-0.03	[18], [19]
$E_{1/2}$ by spectropotentiometry in wet MeCN [c]	---	+1.30	+1.47	[18]
E_{red} from ferrocene titrations [d]	+0.39	+0.51	+0.49	[20]
$[Fe^{II}(bpy)_3]^{2+}$ titrations in the presence of Sc^{III} [e]	---	+1.35	---	[7]

[a] All potential values are vs. SCE. [b] $E_{p,c}$ values obtained from cyclic voltammetry of Fe^{IV}=O complexes in anhydrous MeCN. [c] From spectropotentiometry starting with Fe(II) complexes in MeCN with water. [d] From titrations of Fe^{IV}=O complexes with ferrocenes. [e] From titration of **2** with $[Fe^{II}(bpy)_3]^{2+}$ in the presence of >1000 equiv. $Sc^{III}(OTf)_3$ in MeCN.

The effect of added nitrate ion has also been investigated, as the crystal structure of **3** shows the Ce^{IV} center to have four κ^2-bound nitrate ligands (Figure 3) and the $Ce^{III}(NO_3)_3$ reductant introduced only has three nitrates. Indeed, with the addition of one equiv. $Bu_4N(NO_3)$, both **2** and **4** can be fully converted to **3** and **5**, respectively, with just one equiv. $Ce^{III}(NO_3)_3$ (Figures 4 and S16), demonstrating that the coordination of four nitrates to the Ce^{IV} center stabilizes the Fe^{III}–O–Ce^{IV} species. We interpret these results to indicate a decrease in the $Ce^{IV/III}$ potential upon binding of the fourth nitrate, a notion confirmed by cyclic voltammetry (Figure S21). Importantly, the requirement for only one equiv. $Ce^{III}(NO_3)_3$ shows that the speciation in the solution corresponds precisely to what has been demonstrated by X-ray crystallography (Figure 3).

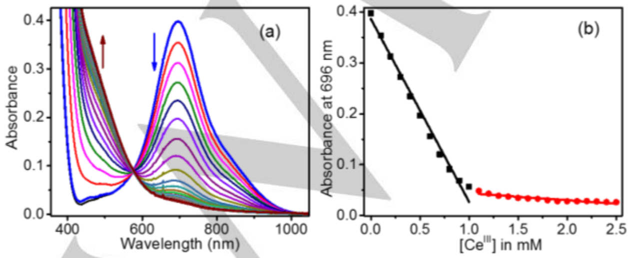

Figure 4. (a) UV-Vis spectral changes observed upon titration of 1 mM **2** ($A_{696\text{-}nm}$ = 1) and 1 equiv. $Bu_4N(NO_3)$in MeCN with 0.1-equiv. aliquots of $Ce^{III}(NO_3)_3$ in MeCN. (b) Plot of A(696 nm) as a function of $Ce^{III}(NO_3)_3$ concentration.

To put the reactions of **2** and **4** with $Ce^{III}(NO_3)_3$ into a broader context, we added $Ce^{III}(NO_3)_3$ to $[(TMC)Fe^{IV}{=}O]^{2+}$ (**1**) in acetonitrile but observed no reaction even with a 20-fold excess of Ce^{III} or with added nitrate. These observations suggest that **1** is a significantly weaker oxidant than **2** or **4**, consistent with the observed reactivities of these three complexes with respect to H-atom and O-atom transfer.[18],[19] On the other hand, Bakac has reported that $[(H_2O)_5Fe^{IV}{=}O]^{2+}$ irreversibly oxidizes $Ce^{III}(NO_3)_3$ ($Ce^{IV/III}$ 1.45 V vs. SCE) in 1 M $HClO_4$.[21] Based on this comparison, the relative oxidizing power of these Fe^{IV}=O complexes decreases in the order: $[(H_2O)_5Fe^{IV}{=}O]^{2+} >> $ **4** > **2** > **1**.

Fukuzumi and Nam have studied the fundamental electron transfer properties of ferrocene derivatives to nonheme Fe^{IV}=O complexes and applied the Nernst equation under equilibrium conditions to determine the reduction potentials of **1**, **2**, and **4** to be about 0.4-0.5 V vs SCE (Table 1).[20] While this approach allowed the redox potentials of these three nonheme Fe^{IV}=O complexes to be compared for the first time, a potential concern is whether a true equilibrium can be established under the experimental conditions, because of the instability of the reduced Fe^{III}–O^{-} species.[22] In contrast, the reduction of **2** and **4** by $Ce^{III}(NO_3)_3$ reported here is facile and reversible, suggesting that **2** and **4** must be relatively close to $Ce^{III}(NO_3)_3$ in redox potential in MeCN solvent. As shown in Figure S21, the $Ce^{IV/III}$ potential of $Ce^{III}(NO_3)_3$ can be tuned between 1-1.3 V vs. SCE by adjusting the Ce:NO_3 ratio.[23] At a 1:4 Ce:NO_3 ratio, 1 equiv. Ce^{III} is sufficient to reduce **2** and **4** to **3** and **5**, respectively, so **2** and **4** must have redox potentials higher than the Ce^{III} species present in the solution ($E_{1/2}$ > 1 V vs SCE), in agreement with values obtained by spectropotentiometric oxidation of corresponding (N4Py)Fe^{III}–OH and (BnTPEN)Fe^{III}–OH complexes (Table 1).[18]

Because Fukuzumi and Nam have shown that a Lewis acid such as $Sc^{III}(OTf)_3$ can interact with the Fe^{IV}=O unit to increase the $Fe^{IV/III}$ redox potential by 0.84 V,[7] the higher potentials deduced for **2** and **4** from the $Ce^{III}(NO_3)_3$ titration experiments may reflect the Lewis acid effect of Ce(III). We have thus investigated the effect of 1,1'-diacetylferrocene ($Ac_2Fc^{+/0}$), another reductant that has a similarly high redox potential (0.89 V vs. SCE) but cannot act as a Lewis acid. As shown in Figure S22, 1 equiv. 1,1'-diacetylferrocene can in fact reduce **2** and **4**, corroborating the high potentials deduced for **2** and **4** and excluding the Lewis acid argument to rationalize the high potentials deduced from the $Ce^{III}(NO_3)_3$ titrations. However, despite having a lower redox potential than $Ce^{III}(NO_3)_3$, Ac_2Fc reduces **2** and **4** much more slowly, requiring 20 min to reduce **4** completely at 20 °C and ten times longer for **2**. This comparison suggests that the Lewis acid does not affect the thermodynamics of the reduction but instead enhances its kinetics presumably by proceeding via a mechanism different from that for Ac_2Fc reduction. The latter very likely occurs by outer-sphere electron transfer, but the Ce(III) reductant offers the possibility of an inner-sphere pathway for electron transfer by coordinating to the $Fe^{IV}(O)$ unit, an intriguing notion we will further investigate in future work.

In this work, we have demonstrated the synthesis of Fe^{III}–O–Ce^{IV} complexes from the reactions of their Fe^{IV}=O precursors with $Ce^{III}(NO_3)_3$ in what turns out to be a facile and reversible transformation. The position of this equilibrium depends on the number of nitrate ligands on the Ce center as controlled by the MeCN/H_2O ratio in the solvent, which tune the $Ce^{IV/III}$ potential.

These observations imply that the $Fe^{IV}=O$ centers of **2** and **4** have reduction potentials higher than that of the Ce^{III} reductant in MeCN (~1 V vs SCE). More importantly, the existence of **3** and **5** supports the formation of analogous Fe–O–Ce adducts in Fe-catalyzed water oxidation as proposed by Lloret-Fillol and Costas.[4] Our work corroborates the assignment of an observed Raman band at 677 cm^{-1} in Fe-catalyzed water oxidation to an Fe–O–Ce intermediate that facilitates formation of the O–O bond, suggesting that CAN may also play such a role in water oxidation reactions catalyzed by other metal complexes. Lastly, despite being a formally spin-forbidden transformation, the conversion of an S = 1 $Fe^{IV}=O$ complex to the corresponding (S = 5/2 Fe^{III})–O–Ce^{IV} species upon addition of Ce^{III} is remarkably facile, being instantaneous even at -40 °C (Figure S23). This observation suggests that the barrier for such spin crossover events at $Fe^{IV}=O$ centers is quite low, an aspect discussed in a recent review by Harvey on computational insights into spin forbidden reactions.[24] Furthermore, this Ce-based conversion bears some analogy to the conversion of an S = 1 $Fe^{IV}=O$ complex to an S = 5/2 Fe^{III}–OH species in an H-atom transfer (HAT) reaction, with Ce^{III} and H• performing similar functions and is fundamentally different from metal-coupled electron transfer (MCET) reactions of $Fe^{IV}=O$ centers in the presence of Lewis acids where the electron does not originate from the Lewis acid, but rather an external reducing equivalent.[25] Assuming this comparison to be valid, little or no barrier may be expected for the S = 1 $Fe^{IV}=O$ reactant to undergo spin-crossover as it initiates HAT. We therefore conjecture that, for S = 1 $Fe^{IV}=O$ centers, it is not the ability to undergo spin crossover that dictates which spin surface is relevant to its HAT reactivity, but rather the gap between the S = 1 ground state and the S = 2 excited state, as invoked in the Two-State Reactivity model of Shaik[10] and recently demonstrated by the correlation of HAT rates with spin state splitting energies for a series of eleven $Fe^{IV}=O$ complexes supported by the tetramethylcyclam ligand.[26]

Experimental Section

Experimental Details. ***Caution!*** *Perchlorate salts of metal complexes are potentially explosive. These compounds should be prepared in small quantities and handled with care.[27]* See the Supporting Information for experimental details of synthesis and physical methods.

Acknowledgements

This work was supported by a grant from the U. S. National Institutes of Health (GM-38767 to L.Q.). XAS data were collected at the Stanford Synchrotron Radiation Lightsource, which is supported by the U.S. DOE under Contract No. DE-AC02-76SF00515. Use of Beamline 7−3 is supported by the DOE Office of Biological and Environmental Research and the National Institutes of Health, National Institute of General Medical Sciences (including P41GM103393). J.E.M.N.K. thanks the Alexander von Humboldt Foundation for a Feodor Lynen Research Fellowship. We thank Dr. Victor J. Young, Jr. of the University of Minnesota Crystallographic Facility for his valuable advice in the crystallographic analysis.

Keywords: water oxidation • iron oxo • CAN • inner-sphere electron transfer • Fe–O–Ce

[1] a) Y. Umena, K. Kawakami, J.-R. Shen, N. Kamiya, *Nature* **2011**, *473*, 55-60; b) M. Suga, F. Akita, K. Hirata, G. Ueno, H. Murakami, Y. Nakajima, T. Shimizu, K. Yamashita, M. Yamamoto, H. Ago, J.-R. Shen, *Nature* **2015**, *517*, 99-103.

[2] a) X. Sala, S. Maji, R. Bofill, J. García-Antón, L. Escriche, A. Llobet, *Acc. Chem. Res.* **2014**, *47*, 504-516; b) J. D. Blakemore, R. H. Crabtree, G. W. Brudvig, *Chem. Rev.* **2015**, *115*, 12974-13005.

[3] a) S. W. Gersten, G. J. Samuels, T. J. Meyer, *J. Am. Chem. Soc.* **1982**, *104*, 4029-4030; b) W. C. Ellis, N. D. McDaniel, S. Bernhard, T. J. Collins, *J. Am. Chem. Soc.* **2010**, *132*, 10990-10991; c) M. Murakami, D. Hong, T. Suenobu, S. Yamaguchi, T. Ogura, S. Fukuzumi, *J. Am. Chem. Soc.* **2011**, *133*, 11605-11613; d) J. L. Fillol, Z. Codolà, I. Garcia-Bosch, L. Gómez, J. J. Pla, M. Costas, *Nat. Chem.* **2011**, *3*, 807-813; e) D. Hong, S. Mandal, Y. Yamada, Y.-M. Lee, W. Nam, A. Llobet, S. Fukuzumi, *Inorg. Chem.* **2013**, *52*, 9522-9531.

[4] Z. Codolà, L. Gómez, S. T. Kleespies, L. Que, Jr., M. Costas, J. Lloret-Fillol, *Nat. Commun.* **2015**, *6*, 5865.

[5] M. Yagi, M. Kaneko, *Chem. Rev.* **2001**, *101*, 21-36.

[6] E. Y. Tsui, R. Tran, J. Yano, T. Agapie, *Nat. Chem.* **2013**, *5*, 293-299.

[7] Y. Morimoto, H. Kotani, J. Park, Y.-M. Lee, W. Nam, S. Fukuzumi, *J. Am. Chem. Soc.* **2011**, *133*, 403-405.

[8] a) S. Fukuzumi, Y. Morimoto, H. Kotani, P. Naumov, Y.-M. Lee, W. Nam, *Nat. Chem.* **2010**, *2*, 756-759; b) J. Prakash, G. T. Rohde, K. K. Meier, A. J. Jasniewski, K. M. Van Heuvelen, E. Münck, L. Que, Jr., *J. Am. Chem. Soc.* **2015**, *137*, 3478-3481.

[9] a) A. Zhou, S. T. Kleespies, K. M. Van Heuvelen, L. Que, Jr., *Chem. Commun.* **2015**, *51*, 14326-14329; b) A. Zhou, J. Prakash, G. T. Rohde, J. E. M. N. Klein, S. T. Kleespies, A. Draksharapu, R. Fan, Y. Guo, C. J. Cramer, L. Que, Jr., *Inorg. Chem.* **2017**, *56*, 518-527.

[10] a) D. Janardanan, Y. Wang, P. Schyman, L. Que, Jr., S. Shaik, *Angew. Chem. Int. Ed.* **2010**, *49*, 3342-3345; *Angew. Chem.* **2014**, *122*, 3414-3417; b) S. Shaik, *Int. J. Mass spectrom.* **2013**, *354–355*, 5-14; c) D. Schröder, S. Shaik, H. Schwarz, *Acc. Chem. Res.* **2000**, *33*, 139-145; d) S. Shaik, H. Chen, D. Janardanan, *Nat. Chem.* **2011**, *3*, 19-27.

[11] Y.-M. Lee, S. N. Dhuri, S. C. Sawant, J. Cho, M. Kubo, T. Ogura, S. Fukuzumi, W. Nam, *Angew. Chem. Int. Ed.* **2009**, *48*, 1803-1806; *Angew. Chem.* **2009**,*121*, 1835-1838.

[12] C. E. MacBeth, A. P. Golombek, V. G. Young, C. Yang, K. Kuczera, M. P. Hendrich, A. S. Borovik, *Science* **2000**, *289*, 938-941.

[13] a) K. D. Koehntop, J.-U. Rohde, M. Costas, L. Que, Jr., *Dalton Trans.* **2004**, 3191-3198; b) X. Shan, J.-U. Rohde, K. D. Koehntop, Y. Zhou, M. R. Bukowski, M. Costas, K. Fujisawa, L. Que, Jr., *Inorg. Chem.* **2007**, *46*, 8410-8417; c) T. E. Westre, P. Kennepohl, J. G. DeWitt, B. Hedman, K. O. Hodgson, E. I. Solomon, *J. Am. Chem. Soc.* **1997**, *119*, 6297-6314.

[14] G. Roelfes, M. Lubben, K. Chen, R. Y. N. Ho, A. Meetsma, S. Genseberger, R. M. Hermant, R. Hage, S. K. Mandal, V. G. Young, Y. Zang, H. Kooijman, A. L. Spek, L. Que, Jr., B. L. Feringa, *Inorg. Chem.* **1999**, *38*, 1929-1936.

[15] a) A. J. Tasiopoulos, T. A. O'Brien, K. A. Abboud, G. Christou, *Angew. Chem. Int. Ed.* **2004**, *43*, 345-349; *Angew. Chem.* **2004**, *116*, 349-353; b) H. Zhang, L. Duan, Y. Lan, E. Wang, C. Hu, *Inorg. Chem.* **2003**, *42*, 8053-8058; c) T. K. Prasad, M. V. Rajasekharan, *Cryst. Growth Des.* **2006**, *6*, 488-491.

[16] a) Y.-M. So, G.-C. Wang, Y. Li, H. H. Y. Sung, I. D. Williams, Z. Lin, W.-H. Leung, *Angew. Chem. Int. Ed.* **2014**, *53*, 1626-1629; *Angew. Chem.* **2014**, *53*, 1626-1629; b) P. L. Damon, G. Wu, N. Kaltsoyannis, T. W. Hayton, *J. Am. Chem. Soc.* **2016**, *138*, 12743-12746.

[17] T. A. Beineke, J. Delgaudio, *Inorg. Chem.* **1968**, *7*, 715-721.

[18] D. Wang, K. Ray, M. J. Collins, E. R. Farquhar, J. R. Frisch, L. Gomez, T. A. Jackson, M. Kerscher, A. Waleska, P. Comba, M. Costas, L. Que, Jr., *Chem. Sci.* **2013**, *4*, 282-291.

[19] C. V. Sastri, J. Lee, K. Oh, Y. J. Lee, J. Lee, T. A. Jackson, K. Ray, H. Hirao, W. Shin, J. A. Halfen, J. Kim, L. Que, Jr., S. Shaik, W. Nam, *Proc. Natl. Acad. Sci. U.S.A.* **2007**, *104*, 19181-19186.

[20] Y.-M. Lee, H. Kotani, T. Suenobu, W. Nam, S. Fukuzumi, *J. Am. Chem. Soc.* **2008**, *130*, 434-435.

[21] H. Bataineh, O. Pestovsky, A. Bakac, *Inorg. Chem.* **2016**, *55*, 6719-6724.

[22] P. Comba, H. Wadepohl, A. Waleska, *Aust. J. Chem.* **2014**, *67*, 398-404.

[23] G. F. Smith, C. A. Getz, *Ind. Eng. Chem. Anal. Ed.* **1938**, *10*, 191-195.

[24] J. N. Harvey, *WIREs Comput. Mol. Sci.* **2014**, *4*, 1-14.

[25] S. Fukuzumi, K. Ohkubo, Y.-M. Lee, W. Nam, *Chem. Eur. J.* **2015,** *21,* 17548-17559.

[26] J. O. Bigelow, J. England, J. E. M. N. Klein, E. R. Farquhar, J. R. Frisch, M. Martinho, D. Mandal, E. Münck, S. Shaik, L. Que, Jr., *Inorg. Chem.* **2017**, *56*, 3287-3301.

[27] W. C. Wolsey, *J. Chem. Ed.* **1973**, *50*, A335-A337.

Entry for the Table of Contents

COMMUNICATION

Cerium caught in the redox act!

Ce^{III} reacts with Fe^{IV}(O) complexes in MeCN to form inner-sphere Fe^{III}–O–Ce^{IV} adducts, a transformation easily reversed by adding water. This facile equilibrium is tuned by the nature of the ligands on the Ce center, and its existence shows that the Ce$^{IV/III}$ and Fe$^{IV/III}$ potentials must fall within a range of 0.9 - 1.1 V vs SCE.

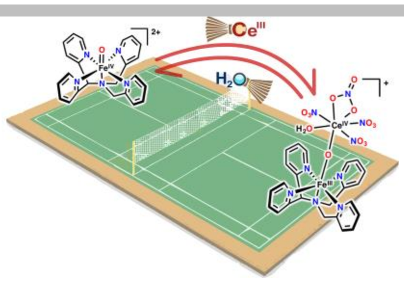

*Apparao Draksharapu, Waqas Rasheed, Johannes E. M. N. Klein, Lawrence Que, Jr.**

Page No. – Page No.

Facile and reversible formation of Fe^{III}–O–Ce^{IV} adducts from nonheme oxoiron(IV) complexes and Ce(III).